ISSN 1674-1056
http://cpb.iphy.ac.cn
http://iopscience.iop.org/cpb
中国物理 B Chinese Physics
中国物理 Chinese Physics B

Spin detection and manipulation with scanning tunneling microscopy

Chunlei Gao(高春雷)

Citation: Chin. Phys. B . 2018, 27(10): 106701. **doi:** 10.1088/1674-1056/27/10/106701

Journal homepage: http://cpb.iphy.ac.cn; http://iopscience.iop.org/cpb

What follows is a list of articles you may be interested in

Liquid phase epitaxy magnetic garnet films and their applications

Yi-Heng Rao(饶毅恒), Huai-Wu Zhang(张怀武), Qing-Hui Yang(杨青慧), Dai-Nan Zhang(张岱南), Li-Chuan Jin(金立川), Bo Ma(马博), Yu-Juan Wu(吴玉娟)

Chin. Phys. B . 2018, 27(8): 086701. **doi:** 10.1088/1674-1056/27/8/086701

Surface effects on the thermal conductivity of silicon nanowires

Hai-Peng Li(李海鹏), Rui-Qin Zhang(张瑞勤)

Chin. Phys. B . 2018, 27(3): 036801. **doi:** 10.1088/1674-1056/27/3/036801

Effect of isotope doping on phonon thermal conductivity of silicene nanoribbons: A molecular dynamics study

Run-Feng Xu(徐润峰), Kui Han(韩奎), Hai-Peng Li(李海鹏)

Chin. Phys. B . 2018, 27(2): 026801. **doi:** 10.1088/1674-1056/27/2/026801

Thermoelectric properties of two-dimensional hexagonal indium-VA

Jing-Yun Bi(毕京云), Li-Hong Han(韩利红), Qian Wang(王倩), Li-Yuan Wu(伍力源), Ruge Quhe(屈贺如歌), Peng-Fei Lu(芦鹏飞)

Chin. Phys. B . 2018, 27(2): 026802. **doi:** 10.1088/1674-1056/27/2/026802

Light-matter interaction of 2D materials: Physics and device applications

Zi-Wei Li(李梓维), Yi-Han Hu(胡义涵), Yu Li(李瑜), Zhe-Yu Fang(方哲宇)

Chin. Phys. B . 2017, 26(3): 036802. **doi:** 10.1088/1674-1056/26/3/036802

TOPICAL REVIEW — Spin manipulation in solids

Spin detection and manipulation with scanning tunneling microscopy*

Chunlei Gao(高春雷)†

State Key Laboratory of Surface Science and Department of Physics, Fudan University, Shanghai 200433, *China*

(Received 1 May 2018; revised manuscript received 12 August 2018; published online 10 September 2018)

Over the past few decades, spin detection and manipulation at the atomic scale using scanning tunneling microcopy has matured, which has opened the possibility of realizing spin-based functional devices with single atoms and molecules. This article reviews the principle of spin polarized scanning tunneling microscopy and inelastic tunneling spectroscopy, which are used to measure the static spin structure and dynamic spin excitation, respectively. Recent progress will be presented, including complex spin structure, magnetization of single atoms and molecules, as well as spin excitation of single atoms, clusters, and molecules. Finally, progress in the use of spin polarized tunneling current to manipulate an atomic magnet is discussed.

Keywords: spin-polarized STM, inelastic tunneling spectroscopy, atomic spin detection

PACS: 67.30.hj, 67.60.gc, 68.65.–k **DOI:** 10.1088/1674-1056/27/10/106701

1. Introduction

With the diminishing size of structures used for information recording and processing, atomic scale functional devices have also become smaller. One plausible route is the use of spin instead of charge on the atomic scale. Owing to advances in spin sensitive techniques with atomic resolution based on scanning tunneling microscopy (STM), remarkable progress has been made in the past decade regarding the detection and manipulation of atomic or molecular magnetic units. This topic includes three parts: measurement of static spin structure or magnetization, dynamic spin properties, and spin manipulation with current injection from the tip. The resolving spin structure on the atomic scale was realized by spin-polarized STM (SPSTM), which has proven its powerful capabilities in many complex magnetic systems, including ferromagnets and antiferromagnets. Combined with an external magnetic field, SPSTM was also used to measure the magnetization of islands, clusters, molecules, defects, and even single atoms. Secondly, knowledge of the stability and dynamics at the surface of a magnetic system was obtained by inelastic tunneling spectroscopy, which corresponds to the energy lost to the magnetic system during the tunneling process. Spin wave excitation and the spin flipping process can all be measured on the atomic level with STM. Finally, controllable manipulation of an atomic magnetic system can be performed with an STM tip. In this review, I will first discuss the technical development of atomic spin detection and manipulation, followed by recent advances in this area.

2. Techniques of spin detection and manipulation with STM

Atomic level spin detection includes static spin-polarized and dynamic spin excitation measurements. A static measurement mainly yields the spin structure and the coercive field in an atomic magnetic system. Spin excitation yields the spin wave dispersion, spin flipping energy, and magnetic stability of magnetic thin films, clusters, molecules, and single atoms.

2.1. Spin-polarized scanning tunneling microscopy

Spin-polarized STM is based on the tunneling magnetoresistance effect; this mature technique uses a magnetic tip and was first described by Wiesendanger *et al.* in 1990.[1] Later, SPSTM was developed into three different operation modes, i.e., constant current mode, spectroscopy mode, and differential magnetic mode. Scanning tunneling microscopy is usually conducted in the constant current mode, i.e., the tunneling current is kept constant by adjusting the vertical position of the tip as the tip scans across the surface. In this case, the contour of the surface electronic structure is mapped, which is defined as the topography. When a ferromagnetic tip forces electrons to tunnel through a sample, the tunneling current contains mixed nonmagnetic and magnetic contributions that govern the topography. When the magnetic part is much smaller than the nonmagnetic part, or specific magnetic states are interested, SPSTM can be operated in the spectroscopic mode. The local differential conductivity is measured, which is proportional to the local density of states (LDOS). The bias voltage can be

*Project supported by the National Natural Science Foundation of China (Grant Nos. 11427902 and 11674063) and the National Key Research and Development Program of China (Grant No. 2016YFA0300904)

†Corresponding author. E-mail: clgao@fudan.edu.cn

© 2018 Chinese Physical Society and IOP Publishing Ltd

chosen to maximize the ratio of magnetic LDOS over nonmagnetic LDOS. Neither the constant current mode nor the spectroscopic mode can separate the nonmagnetic and magnetic contributions to the tunneling current. A complete separation was realized in the differential magnetic mode, which was developed in 1999.[2] When the magnetization direction of the tip (or sample) is switched periodically, the tunneling current oscillates at the same frequency. A change in the tunneling current upon reversal of magnetization is defined as differential magnetic conductivity, which can be extracted with a phase-sensitive lock-in amplifier. In this case, the measured spin signal is proportional to the magnetic part of the integrated LDOS. A more detailed description of SPSTM and its accomplishment can be found in the review by Bode in 2003[3] and Wiesendanger in 2009.[4]

In addition to SPSTM using a magnetic tip, Eltschka *et al.*[5] proposed a method for measuring the absolute spin polarization of a magnetic system with a superconducting tip based on the Meservey–Tedrow–Fulde effect. They successfully resolved the spin polarization of Cobalt islands, and determined the dependence of the spin polarization on the width of the tunneling barrier resulting from different decay rates of electron orbitals into a vacuum.

2.2. Inelastic scanning tunneling spectroscopy

The dynamic properties of a magnetic system can also be obtained in STM geometry through inelastic scanning tunneling spectroscopy (ISTS) measurements. In ISTS, tunneling electrons inelastically interact with one of the electrodes.[6] When the tunneling electrons have enough kinetic energy to excite an inelastic process, the tunneling current I is enhanced due to an increase in the number of final states. The onset of the inelastic scattering process creates a step in the differential conductivity $\mathrm{d}I/\mathrm{d}U$ or a peak in the $\mathrm{d}^2I/\mathrm{d}U^2$ curve. Inelastic excitations may occur in the forward and backward tunneling direction, leading to peaks in the $\mathrm{d}^2I/\mathrm{d}U^2$ curve with odd symmetry in U, which could be treated as a signature of the inelastic process. The energetic loss of tunneling electrons can occur via different processes in the system such as excitons, phonons, or magnons. Spin flip or a spin wave can be excited and quantitively measured in a magnetic system. The magnetic-related inelastic process can be distinguished from a nonmagnetic process (e.g., exciton or phonon formation) with a field-dependent measurement. The magnetic anisotropy of single atoms could be mapped three-dimensionally in this way.[7] A magnetic field-dependent measurement could also reveal the g factor on the atomic scale, as observed by Liu *et al.*[8] within a single magnetic molecule via the extended Kondo effect.

2.3. Spin manipulation

Controllable manipulation of a magnetic system can be realized via an external magnetic field or directly via spin torque transfer by exciting a spin-polarized current. STM can be combined with an external three-dimensional magnetic field. The magnetization direction can be controlled with the external field. However, when the magnetic system approaches the atomic limit, magnetization is stabilized by strong magnetic anisotropy, which is generally much larger than the external magnetic field itself. In this case, hot electrons can be used to excite the system and change the magnetic states of an atomic magnet by injecting energy into the system and inducing the flipping process. Nevertheless, this process has no directional preference, which can be broken by introducing an external field or using a magnetic tip. In the case of an external magnetic field, the hot electrons excite the system and subsequently relax to magnetic states determined by the external field. The external field can also be replaced by an exchange field. In the case of a magnetic tip, additional spin torque can be transferred to the magnetic system, which favors directional atomic magnetic manipulation. Alternatively, spin states of a single atomic or molecular system can also be changed by absorbing and desorbing foreign adsorbates.[9,10]

3. Magnetic structure and magnetic excitation

The behavior of a magnetic system is governed by its static magnetic structure and dynamic response. STM provides the ultimate spatial resolution that was not possible with most traditional techniques, regardless of whether neutrons, electrons, or light was used as the probe. SPSTM was used to measure the spin structure of various magnetic systems ranging from ferromagnetic and antiferromagnetic thin films to magnetic islands, clusters, molecules, or even single atoms. These magnetic systems are not restricted to those with a simple linear magnetic structure. Complex noncollinear spin structure can also be exclusively determined on the atomic scale by combining SPSTM with an external magnetic field. Moreover, the dynamic response of all the above magnetic systems can be obtained by measuring spin excitation with STM.

3.1. Spin structure

3.1.1. Collinear ferromagnets and antiferromagnets

In ferromagnets or antiferromagnets made of a single or a few atomic layers, domain walls can be as sharp as a few atomic lattices, which are only accessible by SPSTM. Pratzer *et al.*[11] measured the ultra-sharp domain walls of monolayer and double layer Fe grown on W(110). The magnetization direction of monolayer Fe is in-plane, while double layer Fe has an out-of-plane easy axis. When measuring with an in-plane sensitive magnetic tip, monolayer Fe shows oppositely

magnetized domains separated by a domain wall as narrow as 0.6 nm, while double layer Fe does not show any magnetic contrast except at the domain wall region where the magnetization direction is tilted into the plane. This kind of sharp domain was also observed in layer-wise antiferromagnets. In general, the domain wall in an antiferromagnet is unfavored, which is usually accompanied by magnetic or structural defects. Schlickum *et al.*[12] observed domain walls in layer-wise antiferromagnet Mn thin films induced by the atomic step of the Fe substrate. The magnetization directions of Mn are either parallel or antiparallel to the magnetization direction of the underlying Fe. On the surface, neighboring Mn terraces have the opposite magnetization direction. Thus, a frustrated region will be formed if an Fe atomic step is present underneath the Mn terraces. Neighboring Mn terraces show magnetic contrast that is clearly visible.[13] In addition, the underlying Fe step creates magnetic contrast within a given Mn terrace. The width of the transition region can be directly measured, which increases from 2 to 7 nm as the thickness of Mn increases.[12]

SPSTM also provides the capability to resolve the antiferromagnetic structure on the atomic scale, especially when operating in constant current mode. Corrugation of the surface magnetic superstructure decays much slower into a vacuum than the atomic structure;[14] thus, the antiferromagnetic structure can be easily resolved with a magnetic tip. As an example, Bode *et al.*[15] observed a checkboard antiferromagnetic spin structure in an Mn monolayer on W(001). Even an atomically sharp antiferromagnetic domain wall induced by structural defects was resolved. In fact, SPSTM was very successful in resolving magnetic states on the atomic scale. These results were cited in the very thorough review by Wiesendanger.[4] Recently, STM was used in many new quantum systems. Enayat, *et al.*[16] found a double-row antiferromagnetic structure in $Fe_{1+y}Te$, which is important in understanding the relationship between ubiquitous antiferromagnetism in parent compounds and their superconducting phase. Hänke *et al.*[17] further studied the reorientation of magnetic moments at the surface compared to bulk $Fe_{1+y}Te$. Yang *et al.*[18] studied magnetism of a magnetically doped topological insulator and found the surface states exhibit ferromagnetism owing to the energy resolution provided by SPSTM.

3.1.2. Nonlinear spin structure

Beyond a simple collinear spin structure, noncollinear spin states are more common. The first class of noncollinearity originates from the topological arrangement of atoms, where the simple antiparallel alignment of neighboring atoms cannot be fully satisfied.[19] These noncollinear states are more probable in more complex crystals. The second class of noncollinear spin states arises from higher order effects involving spin and orbital moments. The relativistic spinorbit coupling may lead to mixing of spin states and as a consequence to noncollinear states. Aside from the magnetocrystalline anisotropy, a well-known effect of spin–orbit coupling in systems with broken inversion symmetry is the anisotropic exchange or Dzyaloshinsky–Moriya interaction.[20,21] This additional term may lead to a non-collinear ground state. A single measurement is insufficient to distinguish between a collinear and a non-collinear spin state. Instead, this requires a combination of spin configuration measurements with different quantization axes.

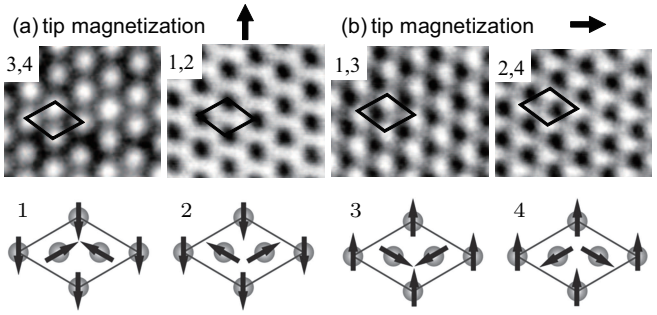


Fig. 1. Four possible configurations of the 120° Néel structure (1, 2, 3, and 4). Panels (a) and (b) are two groups of constant current images taken with magnetic tips. The size of the images is about 2 nm×2.5 nm. By assuming the magnetic orientation of the tip, projections of the four spin configurations on the tip magnetization direction results in different magnetic images.

The classical example of topologically-driven noncollinear antiferromagnetic spin structure is an arrangement of antiferromagnetic atoms in a two-dimensional hexagonal lattice. In this lattice, it is impossible to align all the nearest neighbors such that they are antiparallel. Thus, a frustrated antiferromagnetic Néel structure with a 120° angle between neighboring magnetic moments forms, as shown in Fig. 1. Four energetically degenerate configurations of the 120° Néel structure were drawn and can be distinguished by the orientation of their moments. Direct experimental observation of this Néel structure was found in an Mn monolayer grown on Ag(111).[22] The magnetic contribution in a constant current SPSTM image is proportional to the projection of the spin polarization of the sample on the spin polarization of the tip. If these spin structures are now imaged with a spin polarized tip, four different images can be obtained. If the tip spin polarization is parallel to that of one of the Mn atoms (Fig. 1(a)), the projection of four possible spin configuration results in two kinds of spin images with opposite contrast (Fig. 1(a)). In both images, the spin pattern shows six-fold rotational symmetry. If the tip spin polarization is perpendicular to one of the Mn moments (Fig. 1(b)), three atoms in the unit cell yield three different projections of their spin polarization on the tip spin polarization, thus leading to patterns with only three-fold rotational symmetry (Fig. 1(b)). This unambiguously demonstrates the 120° Néel structure in a monolayer Mn with a triangular lattice.[23]

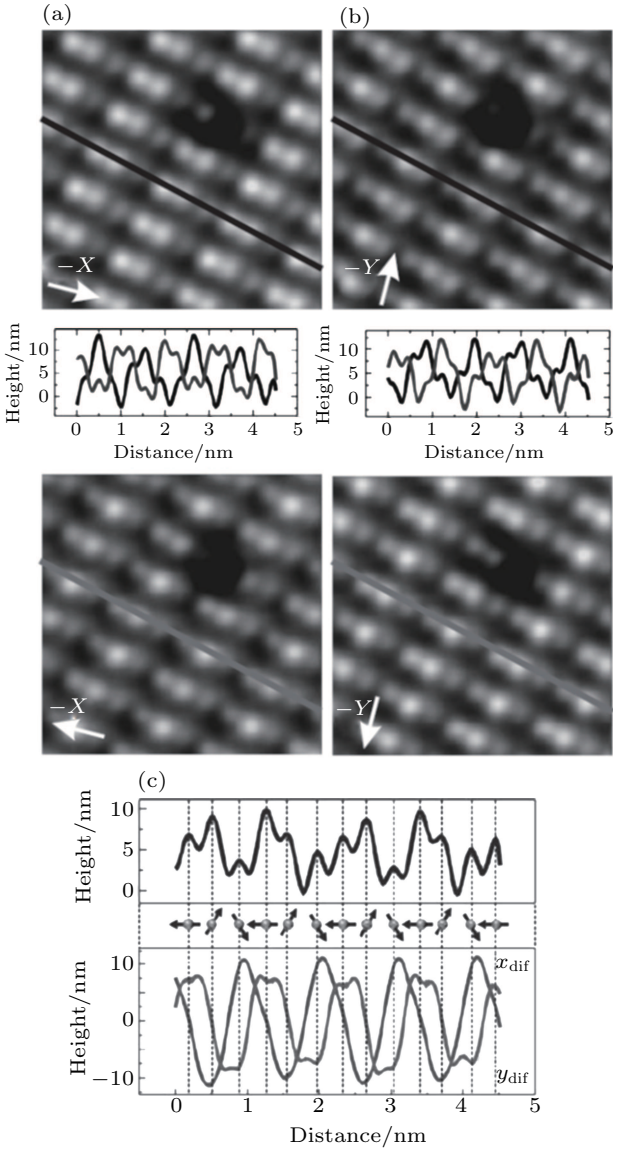


Fig. 2. (a) and (b) Topographical images of a 4 nm×4 nm region under an external field of $X = +2T$, $X = -2T$, $Y = +2T$, and $Y = -2T$, as marked in the images. Line profiles were drawn in the middle of panels (a) and (b). (c) The upper figure shows the topographic profile. The lower figure shows the magnetic components obtained by calculating the difference between the X and Y images. Arrows in the middle show the spin direction of each atom by taking a vector sum of the X and Y magnetic components.

Due to the nonproportional projection of the magnetic moments on different orientations of the noncollinear spin structure, it is quite straightforward to distinguish a noncollinear spin structure from a collinear spin structure. Similar or even more complex noncollinear spin structures have been observed in many topologically driven frustrated systems, such as Cr/Pd(111),[24] Fe/Re(0001),[25] Fe/Ir(111),[26] and Fe/Rh(001).[27] Nevertheless, determining the exact orientation of each atomic magnetic moment is rather challenging. The problem was solved by integrating SPSTM with a 3D external magnetic field. The magnetization direction of the ferromagnetic tip can be rotated to an arbitrary direction with the external field, which then can yield the 3D projection of the atomic magnetic moments. Figure 2 show an SPSTM image of a hexagonal FeSe surface, which is an antiferromagnetic semiconductor. When imaged with an Fecoated W tip, the magnetization direction can be aligned to the external magnetic field, thus yielding different SPSTM images. Taking Fig. 2(a) as an example, the contrast reverses when the tip magnetization changes from the $+X$ to X direction. This can be seen from the line profiles in the two images, which were gathered along the same trajectory in each image. The apparent height difference between three neighboring atoms changes when the tip magnetization is reversed, indicating the spin polarization projected on the magnetization of the tip changes. A similar argument can also be applied to the Y and Z axes. Obviously, $+Y$ and $-Y$ images (Fig. 2(b)) also contain a large spin contribution. The appearance of the SPSTM images along the X direction are different from the images gathered along Y direction, indicating that the projection of spin polarization along X is not proportional to that on Y. This means that the surface has a noncollinear spin structure, while in the Z axis, the $+Z$ image is nearly the same as the $-Z$ image (not shown, see Ref. [28]), indicating a negligible spin polarization in the Z direction. This can also be seen from the corresponding line profiles. Thus, the spin orientation of individual atoms can be determined by vectorially adding the X and Y components, as shown in Fig. 2(c).

Strong spin–orbit coupling could also induce a complex spin structure. A single Mn monolayer on the pseudohexagonal surface of W(110) was firstly found to have row-wise antiferromagnetic order.[29] Interestingly, later on, a more detailed study found that there is a large scale periodic modulation of the contrast with a 6 nm period superimposed on the row-wise contrast.[30] Interestingly, the observed SPSTM images change with the application of the external magnetic field. The areas of maximal corrugation move laterally excluding a spin density wave, thus implying that the spin structure is a non-collinear spiral. *Ab initio* calculations including the spin–orbit interaction indicate that the ground state of Mn on W(110) is indeed a cycloidal spin spiral.[30] Nevertheless, it is difficult to determine the direction of the spin spiral without the in-plane directional sensitivity; on the other hand, this shows the importance of the vector field. Meckler *et al.*[31] studied the magnetic structure of an Fe double layer on W(110) and found an inhomogeneous right-rotating cycloidal spin spiral that was not observed in the SPSTM measurement.[11] There are only a few SPSTM instruments with vector fields that currently exist; some of these were recently developed and could facilitate measurements at temperatures as low as 25 mK,[32] or could allow rotation of the scanning head rather than rotating the field.[33] It is certain that SPSTM combined with ultralow temperature and a vector field has unique advantages in studying complex magnetic properties.

3.1.3. Molecules, defects, and single atoms

SPSTM was not only applied to research into ferromagnetic or antiferromagnetic structures, but was also successfully used to investigate the magnetization of single molecules, defects, and atoms, which are promising building blocks for next generation magnetic functional devices on the atomic scale. The atomic resolution of SPSTM has a natural advantage in studying these nanoscale objects, including single molecules,[34–37] dopants[38] or defects,[39] and single atoms.[40,41]

Figure 3 shows an SPSTM measurement of an iron porphyrin (FePc) molecule.[34] In this experiment, FePc was grown on Bi_2Te_3, resulting in the formation of a flat molecular layer. Figure 3(a) shows a detailed image of one FePc molecule, where the central Fe atoms and four ligands are clearly visible. dI/dV curves (Fig. 3(b)) taken under opposite magnetic fields clearly show that Fe is spin-polarized. Magnetic hysteresis loops can be obtained by plotting the dI/dV magnitude as a function of the applied field, with the magnetic field parallel and perpendicular to the film, as shown in Figs. 3(c) and 3(d), respectively. The overlap of the dI/dV value when increasing and decreasing the field in both cases clearly shows paramagnetic behavior. The saturation field is, however, very different. The in-plane signal saturates at 0.3 T, while the out-of-plane signal does not saturate until the field strength reaches 3 T. These results clearly indicate that the magnetic moments of FePc when deposited on Bi_2Te_3, and FePc has an in-plane easy axis with a considerably large magnetic anisotropy.

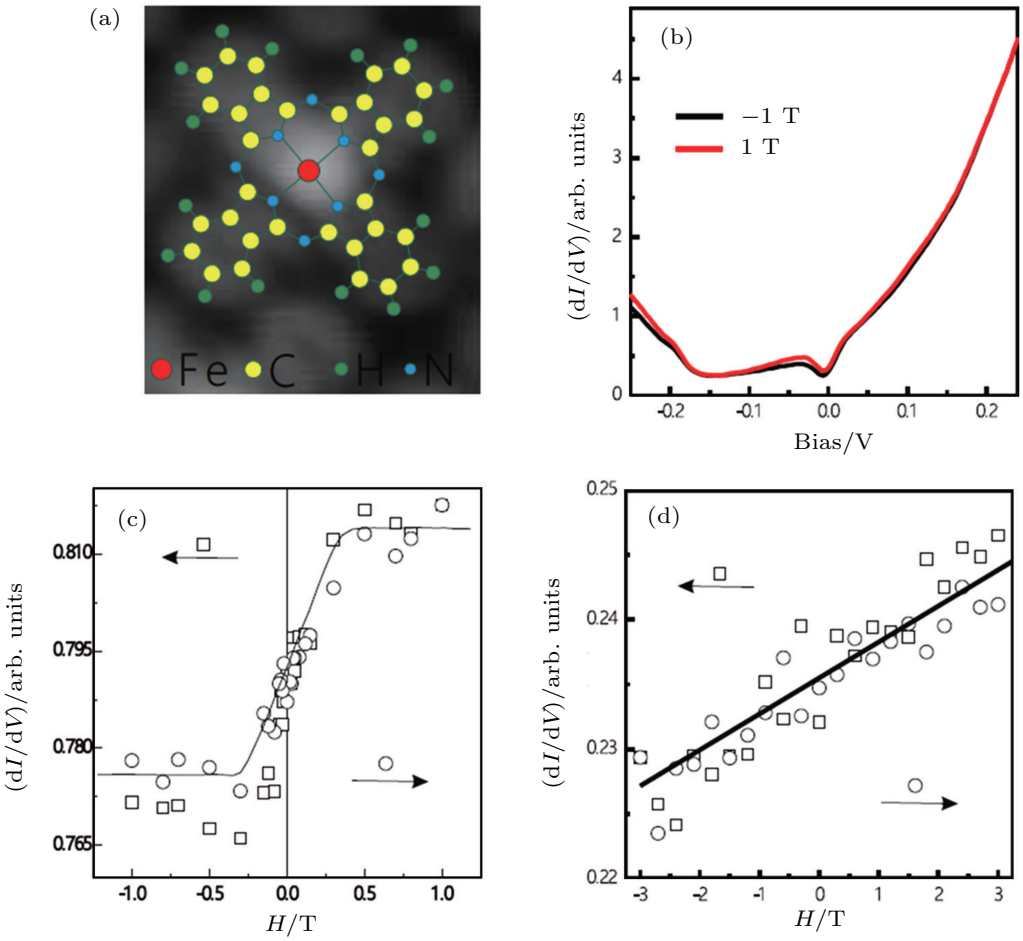


Fig. 3. (color online) (a) Topography of a single FePc molecule where the central Fe atom and four ligands are clearly resolved. (b) dI/dV curves under ± 1 T at the same Fe atom, where the magnetic field is parallel to the *ab* plane. Panels (c) and (d) show dI/dV at a fixed energy versus the magnetic field of the atom with the magnetic field aligned parallel and perpendicular to the *ab* plane, respectively.

SPSTM is not limited to studying molecules, but magnetic defects can also be studied with SPSTM. One can deduce the bulk properties in addition to interesting magnetic properties of defects. Chen *et al.*[39] studied the magnetic properties of an FeSe surface with Se vacancies at the surface. FeSe is the simplest Fe based superconductor whose parent phase is currently under debate. First of all, unlike the obvious antiferromagnetic superstructure observed with SPSTM in a similar system ($Fe_{1-y}Te$[16]), no trace of a magnetic superstructure in the SPSTM images could be observed in FeSe. However, magnetic contrast was observed from Se vacancies, as shown in Fig. 4. Similar to measurement on FePc molecules, as dis-

cussed before, figure 4(a) shows magnetic hysteresis loops in an Se defect, as well as at the bare surface. At the Se site closest to the vacancy, the magnetic loop displays clear paramagnetic behavior under a perpendicular magnetic field (black curve in Fig. 4(a)) while, at the Se site far away from vacancy, the $\mathrm{d}I/\mathrm{d}V$ value does not show any change with the external magnetic field changes (red curve in Fig. 4(a)). From the fact that the magnetization of the Se vacancy follows perfectly with the applied magnetic field, it can be concluded that FeSe thin film is nonmagnetic. If this were not the case, magnetization of the Se vacancy would be pinned by magnetization of the film. Further evidence of a nonmagnetic FeSe thin film is conceived in the spatial distribution of the spin polarization around the Se vacancy. Figures 4(b) and 4(c) show constant current images taken at opposite magnetic fields of ±0.5 T. By subtracting Fig. 4(b) from Fig. 4(c), topographic information was eliminated and a net spin distribution was obtained, as shown in Fig. 4(d). One can see clearly that the four Se sites around the defects manifest nearly the same spin polarization, which is shown in the line profiles (Fig. 4(f)) across the defects. From the perspective of symmetry, the presence of any magnetic superstructure in the Fe layer will break the fourfold symmetry in the spin channel. Thus, FeSe films must be nonmagnetic and magnetization damps rapidly at larger distances from the vacancy, and *ab initio* calculations further confirm that the defects behave as a ferrimagnetic cluster.

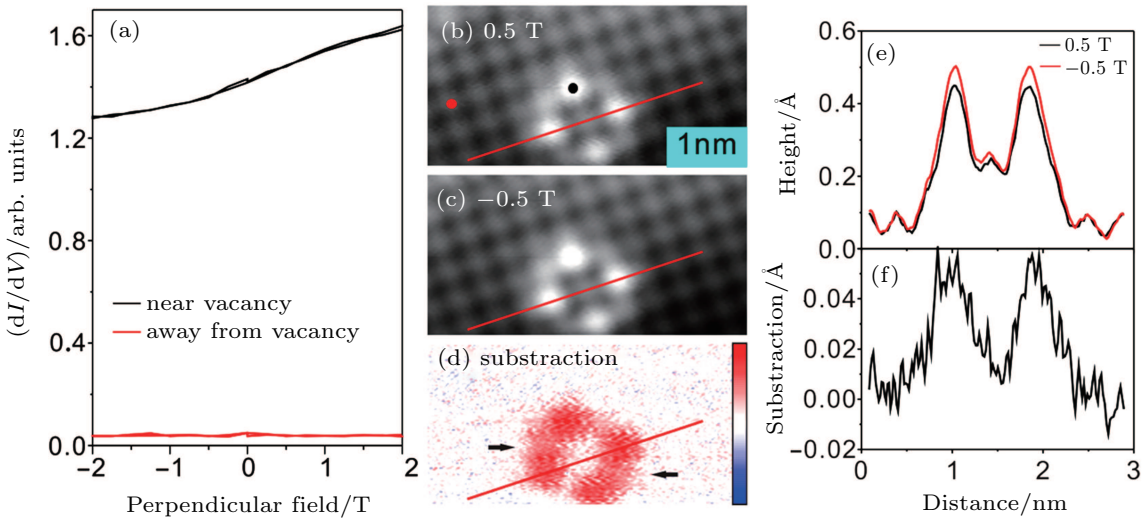


Fig. 4. (color online) (a) Magnetization curve measured with SPSTM near and away from the vacancy. (b) and (c) Topographical images taken with a Cr tip under antiparallel 0.5-T magnetic fields. (d) Difference image of panels (b)–(c). Panels (e) and (f) show line profiles from panels (b), (c), and (d).

Finally, as an example of the magnetization of single atoms, Meier *et al.*[40] investigated single Co atoms on Pt(111). They successfully obtained magnetization curves for single Co atoms, which show paramagnetic behavior even at 0.3 K, although the expected magnetic anisotropy is as high as 9.3 meV per atom. The absence of hysteresis was attributed to the temperature-independent switching process, such as quantum tunneling of magnetization or current-induced magnetization switching by inelastic processes. In addition, they measured the long-range coupling between Co adatoms and the Co monolayer. A damped oscillatory behavior was observed, which is concluded to occur via Ruderman–Kittel–Kasuya–Yosida (RKKY) exchange through conduction electrons in the Pt substrate.

3.2. Spin excitation

In bulk or thin film magnetic materials, spin excitation is the collective motion of magnetic moments, i.e., spin waves or magnon. While most spin wave measurement techniques do not provide any spatial resolution, STM offers the unique capability of measuring spin wave excitation on the atomic scale. On the other hand, when the magnetic unit reduces down to a few or even single atoms, the collective motion of magnetic moments changes to the atomic spin flipping process, which is only observable with STM. All these excitations can be observed with inelastic scanning tunneling spectroscopy measurements, where the tunneling electron loses energy to all possible sorts of excitations in a solid. The key is to distinguish magnetic excitation from other excitations. An external magnetic field and low temperature environment are generally required for ISTS measurements, where the magnetic field can be used to distinguish the magnetic excitation from the nonmagnetic one, while the low temperature environment suppresses thermal fluctuations.

3.2.1. Spin wave excitation

Balashov *et al.*[42] used ISTS to observe magnon excitation in bulk Fe. The excitation energy is of the order of a few meV. To distinguish the origin of the excitation, i.e., magnons or phonons, they used a spin-polarized STM tip as a source

for hot electrons. Depending on the relative orientation of tip and sample spin polarization, the inelastic spectrum is altered while the relative orientation between the tip and sample switched, confirming magnon excitation.

Beyond the lateral resolution, STM can also be used to determine the momenta and life times of magnons by measuring standing spin wave excitation. In bulk magnetic materials, magnons are free to travel in any direction, resulting in a continuous dispersion of magnon energy E as a function of momentum k. Magnons in thin films are confined normal to the film plane, and standing magnons are formed. Their dispersion relation is given by a series of spin wave branches quantized in k_z normal to the film plane, while dispersion is continuous along the k_x and k_y directions. Gao *et al.*[43] measured $\mathrm{d}^2I/\mathrm{d}U^2$ spectra of fcc-Mn ultrathin films on $Cu_3Au(001)$, which is a layer-wise antiferromagnet.[44] In agreement with simple quantization, a series of excitation peaks in the inelastic spectra was observed (Fig. 5(a)). The onset of every branch of standing magnons is observed as a peak in an ISTS measurement. From the thickness t of the Mn layer and the order of the peak, magnon dispersion can be computed using a simple conversion $k_z = n\pi/t$, as shown in Fig. 5(b), which agrees well with neutron scattering data from Nistabilized bulk fcc-Mn and *ab initio* calculations.[43]

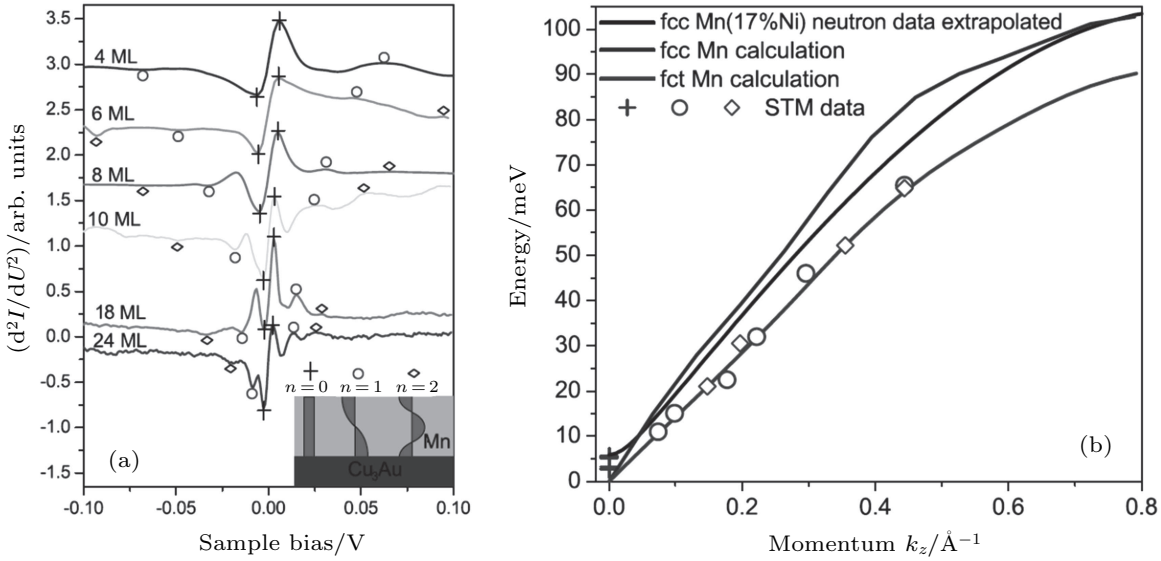


Fig. 5. (a) Thickness dependent inelastic tunneling spectra in Mn thin films. (b) Magnon dispersion curve extrapolated from (a) together with neutron scattering data.

3.2.2. Spin flipping

The single atomic spin-flipping process was first observed by Heinrich *et al.*[45] in 2004 on a single Mn atom on an Al_2O_3 substrate. The substrate is decoupled from a metal by a thin insulating layer, and Zeeman splitting energy can be measured by ISTS. This method was soon extended to other systems, including single atoms on both metallic[46–48] and insulating[49–51] substrates. Magnetic anisotropy energy can be directly obtained through ISTS measurements. The anisotropic energy is usually quite small on a metallic substrate, but it can be enhanced on heavy metals with large spin orbit coupling. The magnetic anisotropy can be significantly increased by hybridizing magnetic atoms with the molecular orbits of insulators. In fact, if a proper insulating layer is chosen, giant magnetic anisotropy energies as large as 58 meV per atom were observed in single Co atoms on a MgO substrate.[49] This striking behavior originates from the dominating axial ligand field at the O adsorption site, which leads to out-of-plane uniaxial anisotropy while preserving the gas-phase orbital moment of Co.

The pursuit of high anisotropic single atomic systems is critical to realizing nanoscopic magnets for high-density magnetic data storage or quantum computing. Despite the high anisotropic energy, which is already far above room temperature, stable magnetization of a single atomic magnet is observable over the order of minutes, even at an extremely low temperature. Quantum mechanical fluctuations are believed to largely dominate the magnetic instability. Decoupling from the thermal bath of electrons, nuclear spins, and lattice vibrations can be reduced by inserting an insulating layer[49–51] or using symmetry protection.[48] It is still possible to further enhance the magnetic anisotropy by using 4d or 5d elements instead of 3d atoms,[52] or by using a specially designed artificial atomic structure, such as a Co or Ir biatomic system on graphene.[53] A recent experiment already shows that Ho on MgO can be stabilized for hours.[54] In this experiment, the authors used single atom electron spin resonance measurements, which are capable of detecting single spins with minimal perturbations.[55]

4. Spin manipulation on the atomic scale

The prerequisite for successful spin manipulation is a stable magnetic system. As can be seen from the previous discussion, isolated magnetic atoms suffer from magnetic fluctuations. Thus far, most experiments were performed in the random switching mode induced by hot (spin-polarized) electrons injection from the tip. Three effects can influence spin manipulation: thermal heating, spin torque transfer, and Oersted field effects.[56,57] While thermal heating has no directional preference, spin torque transfer can change the magnetization to a certain direction. Current-induced switching experiments were performed in paramagnetic islands,[57] clusters,[58,59] or even single atoms.[48,54,60]

Krause *et al.*[57] studied Fe monolayer islands containing about 100 atoms. These islands are ferromagnetic and they found that a tunneling current induced magnetization switching over a time scale of milliseconds. The spin-polarized tunneling current induced an imbalance of the up and down states, indicating that spin torque transfer is playing its role in addition to thermal excitation. The magnetic islands reach the quantum limit when the nanomagnet is only composed of a few atoms. Khajetoorians *et al.*[59] studied 5 exchange-coupled Fe atoms on Cu(001) and found that the magnet switched between two degenerate spin states. The quantum magnet can also be made of an antiferromagnetically coupled cluster. Loth *et al.*[58] built antiferromagnetic atomic single atomic rows of Fe atoms on a Cu_2N overlayer on Cu(001). The tunneling current can induce switching of an energetically equivalent, yet geometrically different Néel state within milliseconds. They also built double atomic rows by atomic manipulation with STM and showed that the extended thermal stability at low temperature makes the system useful for recording information. Single atoms stabilized by high magnetic anisotropy can also be switched by changing the tunneling current. Miyamachi *et al.*[48] studied the stability of Ho single atoms on Pt(111) and reported stable magnetization over a time scale of minutes, which they attributed to symmetry protection, i.e., an effective decoupling from the thermal bath of electrons, nuclear spins, and lattice vibrations by a combination of several symmetries intrinsic to the system. These symmetries include time reversal symmetry, internal symmetries of the total angular momentum, and point symmetry in the local environment of the magnetic atom. Very recently, Natterer *et al.*[54] showed that individual Ho atoms on MgO can retain their magnetic information over many hours and demonstrated the possibility of reading and writing magnetic states in single atomic magnets. Their high magnetic stability combined with controllable manipulation shows that single-atom magnetic memory is indeed possible. Furthermore, Khajetoorians *et al.*[61] demonstrated that it is possible to build a logic circuit with single atoms.

Aside from the above examples of magnetic state manipulation, spin polarized tunneling current was also successfully used in non-traditional spin manipulation methods. Romming *et al.*[62] showed that skyrmions could be deleted or written on a PdFe bilayer on Ir(111). Choi *et al.*[63] showed that a spin-polarized tunneling current can switch the Fe-layer magnetism into a nontrivial C4 (2×2) order on single-crystal Sr_2VO_3FeAs, which cannot be achieved by thermal excitation with an unpolarized current.

5. Conclusion and outlook

This review discusses spin detection and manipulation on the atomic scale with STM. Spin-polarized STM is already a mature technique that is capable of resolving spin states with atomic resolution. It was widely used to detect all kinds of spin structures. In particular, when combined with a vector magnetic field, it can unambiguously determine the magnetic orientation of each atomic moment. Inelastic tunneling spectra were used to study spin excitation in nanoscale objects. This offers the capability to obtain the magnetic anisotropy energy of individual atoms. Highly anisotropic single atom systems were realized in single magnetic atoms on an MgO substrate. Manipulation of the spin states with a spin-polarized tunneling current on the atomic scale can be achieved in a single atomic system with sensitivity and resolution beyond the scope of other techniques. Atomic spin-based information recording and procession are expected to be practical in the future.

References

[1] Wiesendanger R, *et al.* 1990 *Phys. Rev. Lett.* **65** 247
[2] Wulfhekel W and Kirschner J 1999 *Appl. Phys. Lett.* **75** 1944
[3] Bode M 2003 *Rep. Prog. Phys.* **66** 523
[4] Wiesendanger R 2009 *Rev. Mod. Phys.* **81** 1495
[5] Eltschka M, *et al.* 2014 *Nano Lett.* **14** 7171
[6] Wolf E L 1985 *Principles of Electron Spectroscopy* (New York: Oxford University Press)
[7] Yan S, *et al.* 2015 *Nano Lett.* **15** 1938
[8] Liu L, *et al.* 2015 *Phys. Rev. Lett.* **114** 126601
[9] Liu L, *et al.* 2013 *Sci. Rep.* **3** 1210
[10] Stróżecka A, *et al.* 2012 *Phys. Rev. Lett.* **109** 147202
[11] Pratzer M, *et al.* 2001 *Phys. Rev. Lett.* **87** 127201
[12] Schlickum U, *et al.* 2004 *Phys. Rev. Lett.* **92** 107203
[13] Schlickum U 2005 "Spin-polarized scanning tunneling microscopy studies on in-plane magnetization components of thin antiferromagnetic films on Fe(001)", 2005, Thesis
[14] Heinze S, *et al.* 1998 *Phys. Rev. B* **58** 16432
[15] Bode M, *et al.* 2006 *Nat. Mater.* **5** 477
[16] Enayat, M, *et al.* 2014 *Science* **345** 653
[17] Hänke T, *et al.* 2017 *Nat. Commun.* **8** 13939
[18] Yang, F, *et al.* 2012 *Phys. Rev. Lett.* **109** 016801
[19] Anderson P A 1973 *Mater. Res. Bull.* **8** 153
[20] Dzialoshinskii I E 1957 *Sov. Phys. JETP* **5** 1259
[21] Moriya T 1960 *Phys. Rev.* **120** 91
[22] Gao, C L , Wulfhekel, W, Kirschner and J 2008 *Phys. Rev. Lett.* **101** 267205
[23] Wulfhekel W and Gao C L 2010 *J. Phys.: Condens. Matter* **22** 084021
[24] Wasniowska, M, *et al.* 2010 *Phys. Rev. B* **82** 012402
[25] Palacio-Morales, *et al.* 2016 *Nano Lett.* **16** 6252

[26] von Bergmann, K, *et al.* 2006 *Phys. Rev. Lett.* **96** 167203
[27] Takada, M, *et al.* 2013 *J. Magn. Magn. Mater.* **329** 95
[28] Zhang K F, *et al.* 2016 *Appl. Phys. Lett.* **108** 061601
[29] Heinze S, *et al.* 2000 *Science* **288** 1805
[30] Bode M, *et al.* 2007 *Nature* **447** 190
[31] Meckler S, *et al.* 2009 *Phys. Rev. Lett.* **103** 157201
[32] Allworden V, *et al.* 2018 *Rev. Sci. Instrum.* **89** 033902
[33] Trainer, C, *et al.* 2017 *Rev. Sci. Instrum.* **88** 093705
[34] Song Y R, *et al.* 2014 *Phys. Rev. B* **90** 180408(R)
[35] Brede J, *et al.* 2010 *Phys. Rev. Lett.* **105** 047204
[36] Atodiresei N, *et al.* 2010 *Phys. Rev. Lett.* **105** 066601
[37] Schwöbel J, *et al.* 2012 *Nat. Commun.* **3** 953
[38] Khajetoorians A A, *et al.* 2010 *Nature* **467** 1084
[39] Chen W J, *et al.* 2017 *Phys. Rev. B* **96** 214426
[40] Meier F, *et al.* 2008 *Science* **320** 82
[41] Khajetoorians A A, *et al.* 2011 *Phys. Rev. Lett.* **106** 037205
[42] Balashov T, *et al.* 2006 *Phys. Rev. Lett.* **97** 187201
[43] Gao C L, *et al.* 2008 *Phys. Rev. Lett.* **101** 167201
[44] Lin W C, *et al.* 2007 *Phys. Rev. B* **75** 054419
[45] Heinrich A J, *et al.* 2004 *Science* **306** 466
[46] Khajetoorians A A, *et al.* 2013 *Phys. Rev. Lett.* **111** 157204
[47] Hermenau J, *et al.* 2018 *Nano Lett.* **18** 1978
[48] Miyamachi T, *et al.* 2013 *Nature* **503** 242
[49] Rau I G, *et al.* 2014 *Science* **344** 988
[50] Hirjibehedin C F, *et al.* 2006 *Science* **312** 1022
[51] Hirjibehedin C F, *et al.* 2007 *Science* **317** 1199
[52] Ou X D, *et al.* 2015 *Phys. Rev. Lett.* **115** 257201
[53] Hu J and Wu R Q 2014 *Nano Lett.* **14** 1853
[54] Natterer F D, *et al.* 2017 *Nature* **543** 226
[55] Choi T, *et al.* 2017 *Nat. Nanotechnol.* **12** 420‘
[56] Krause S, *et al.* 2011 *Phys. Rev. Lett.* **107** 186601
[57] Krause S, *et al.* 2007 *Science* **317** 1537
[58] Loth S, *et al.* 2012 *Science* **335** 196
[59] Khajetoorians A A, *et al.* 2013 *Science* **339** 55
[60] Serrate D, *et al.* 2010 *Nat. Nano* **5** 350
[61] Khajetoorians A A, *et al.* 2011 *Science* **332** 1062
[62] Romming N, *et al.* 2013 *Science* **341** 636
[63] Choi S, *et al.* 2017 *Phys. Rev. Lett.* **119** 227001